A New Improved Algorithm for Low Complexity Wideband Angle of Arrival Estimation

Bakhtiar A. Karim and Haitham K. Ali
Communication Engineering, Sulaimani Polytechnic University, Sulaimani, Iraq
Email: Bakhtiar.ali@spu.edu.iq; Haitham.ali@spu.edu.iq

Abstract—**The two fundamental problems of Test of Orthogonality of Projected Subspace (TOPS) based Angle of Arrival (AOA) estimation methods are computational complexity and spurious peaks. This work tries to explain the causes of these problems and applies a two-step modification to the Squared-TOPS (SQ-TOPS) procedure to tackle both problems. In the first step, the computational complexity is minimized via replacing the computationally-intensive eigenvalue decomposition (EVD) with a novel Covariance Matrix (CM) subsampling methodology to construct Projection Matrix (PM). Second, the problem of spurious peaks generation is addressed by establishing a new squared orthogonality test between the newly created PM and the transferred signal subspaces (after subspace projection). To justify the effectiveness of the suggested method, a numerical example along with intensive Monte Carlo simulations over different scenarios are provided where the proposed algorithm is systemically compared with its rival methods. The simulation results show the superiority of the proposed algorithm, projection matrix squared TOPS (PMS-TOPS), in terms of lower complexity, higher accuracy, less sensitivity to correlated sources, and low converges time in comparison to TOPS, SQ-TOPS, and weighted square TOPS (WS-TOPS) methods.**

Index Terms—**Angle of arrival, computational complexity, projection matrix, wideband signals**

I. Introduction

Source localization using antenna array has been an attractive research topic due to its potential contribution in various applications such as sonar, radar, wireless communications, and Unmanned Aerial Vehicle (UAV) [1]-[3]. Direction/Angle of arrival (DOA\AOA) estimation is a primary method for both narrowband and wideband sources localizations. The AOA estimation techniques for narrowband sources, such as maximum likely hood (ML), multiple signal classification (MUSIC), estimation of signal parameters via rotational invariance technique (ESPRIT), have been widely studied [4], [5]. These algorithms, however, are not directly applicable to localize wideband sources. The reason for this inapplicability is that narrowband AOA estimation algorithms built based on an assumption that time delays between array elements can be approximated by phase shifts. This assumption, however, is valid only when the signal center frequency (f_c) is significantly high compared to its bandwidth (BW) (i.e., f_c>>BW). In wideband source localization, the phase difference between array sensors is the function of not only AOA, but also temporal frequency of the incident signals [6]. Thus, pre-processing step to decompose the wideband signal into multiple narrowband signals using Discrete Furrier Transform (DFT) is usually required.

Generally, narrowband and wideband AOA estimations involve time-domain and frequency-domain analyses, respectively. The former one seems to be inappropriate for wideband signals as the steering vector is frequency dependent rather than angle dependent only [7]. Additionally, the information within all frequency bins of the wideband signal need to be taken into consideration, thus frequency-domain analysis is required [8]. From the complexity perspective, in contrast to the time-domain analysis of narrowband signals in which array output can easily be represented with a single frequency, direction-finding of wideband signals in frequency-domain is more complex due to processing multiple-frequencies. However, frequency-domain analysis for wideband signals yields higher accurate result compared to the single-frequency analysis in time-domain which may lead to missing existing valuable information in wideband signals [9], [10]. Therefore, in this paper frequency-domain analysis is adopted.

The wideband AOA estimators are generally classified into two categories; Incoherent Signal Subspace (ISS) [11] and Coherent Signal Subspace (CSS) [12] methods. The former one processes all the frequency bins independently then the results of all the bins are averaged to obtain the final AOA estimation. However, poor estimation in one bin will negatively affect the accuracy of the final estimation. Therefore, this method performs well only in the high SNR region. To address this problem, CSS methods are introduced. In this category, an appropriate transformation matrix is used to transfer the covariance matrices (CMs) at different frequencies to a universal CM. The universal CM will have the same structure as narrowband CM at a specific frequency band; hence, it is processed by narrowband AOA algorithms such as MUSIC. Under low SNR condition, CSS methods show better estimation performance than ISS algorithms.

Manuscript received May 5, 2022; revised May 25, 2022; accepted June 2, 2022.

Corresponding author: Bakhtiar A. Karim (email: Bakhtiar.ali@ spu.edu.iq).

doi: 10.18178/ijeetc.11.6.398-409

Two-sided Correlation Transformation (TCT) [13] and Weighted average of signal subspaces (WAVES) [14] are the developed versions of CSS algorithms. However, the requirement for the initial estimation of the signal's direction, known as focusing angle, is the main drawback for CSS methods as their accuracies depend on how close the focusing angle to the true AOA [15].

To address this problem, a new class of wideband AOA estimation named test of orthogonality of projected subspace (TOPS) was introduced [8]. The TOPS algorithm is different from both coherent and incoherent methods and tries to fill the gap between them, therefore, it is known as non-coherent method. The TOPS estimator evaluates the orthogonality between the transferred Signal Subspace (SS) and Noise Subspaces (NS) at different frequencies. The two subspaces are orthogonal only when the hypothesized angle in the transformation matrix equals to the true AOA. The main merit of the TOPS algorithm is that it does not need pre-processing for initial estimation values and performs well at mid SNR. In addition to its high-complexity and false peaks, the performance of this algorithm, however, degrades when wideband sources are correlated. Later, squared TOPS (SQ-TOPS) algorithm [16] was presented which uses SS and NSs twice known as squared test of orthogonality. This modification improves the estimation performance compare to the standard TOPS algorithm, however, at the cost of higher computational complexity. Additionally, SQ-TOPS does not remove false peaks appearing in the TOPS spectrum. To tackle this problem, weighed squared TOPS (WS-TOPS) [17] was proposed. This algorithm eliminates the false peaks and enhances the AOA estimation accuracy through using a new squared matrix and applying the selective weighted averaging process. The performance-enhancement achieved through the WS-TOPS estimator, however, comes at the cost of adding more computational cost.

Current researches in wideband AOA estimation concentrate mainly on two aspects; computational complexity and estimation accuracy. The accuracy of the traditional wideband AOA estimations is directly related to the accuracy of the initial values. Recently, focus on SS(FSS) method is proposed [18] that partially avoids the dependency of the initial values. However, the computational complexity related to the focusing matrix evaluation is not addressed in FSS. Co-prime array configuration is adopted in the latest research [19] to overcome the algorithm complexity. Other works have tried to make the improvement in both aspects [20]-[22]. Furthermore, recent work presented in [23] applies the TOPS algorithm to the coherent sources at the cost of more complexity added by the de-correlation process.

From the above description, there exist two main problems in the TOPS and SQ-TOPS algorithms which are complexity and accuracy. First, the computational complexity of these methods is mainly due to applying eigenvalue decomposition (EVD) technique to each frequency bin to extract subspaces from the measured CM [9], [15]. Second, estimation accuracies of these algorithms are affected by the spurious peaks that makes it difficult to detect true signal directions [24]. The previous works mainly tried to balance the two contradictory aspects, complexity and accuracy (i.e., improving one of them at the cost of the other). Therefore, the improvement in both aspects simultaneously remains challenging and this has motivated the work presented in this paper.

In this work, we aim to tackle these two problems by introducing an enhanced wideband AOA estimation algorithm based on the SQ-TOPS method, so named projection matrix squared TOPS (PMS-TOPS). To this end, the PMS-TOPS algorithm applies two-step modifications to the SQ-TOPS procedure. In the first step, the computationally-inefficient EVD required in each frequency band is replaced by an efficient Projection Matrix (PM) constructed based on a novel sampling methodology that successfully extracts most valuable information from the CM. This step is motivated by the fact that complexity of PM construction is considerably lower than that EVD technique [25]. In addition to reducing the overall computational cost, this substitution guarantees higher estimation accuracy within low and mid SNR regions and makes the algorithm to be less sensitive and more stable against correlated sources. In the second step, the proposed method employs a new squared evaluation matrix and runs the orthogonality test between the transferred SS and the constructed PM for each hypothesized angle. This step will eliminate the false peaks generated mainly due to reinforcing noise components resulted from dot product between NS and the signal null-space [26].

To sum up, we offer the following contributions:

- The proposed PMS-TOPS algorithm enjoys lower complexity compared to the TOPS, SQ-TOPS, and WS-TOPS algorithms. This is achieved by avoiding repeatedly applying the computationally-expensive EVD technique to each frequency band. This achievement leads to minimum computational cost and minimum execution time compared to the counterpart methods and makes it an appropriate choice for limited power applications such as IoT and AUV.
- The PMS-TOPS has minimum sensitivity to the correlated sources and retains high performance in the presence of coherent sources. This is accomplished by applying a new subsampling methodology to construct PMs.
- The introduced method eliminates the false peaks appearing in the TOPS and SQ-TOPS spectrums. This improvement is obtained by employing a new squared orthogonality evaluation matrix and avoiding noise-compounding effect.

This paper is organized as follows. Wideband signal model and problem formulation are described in Section II. Section III reviews some of the most related works. In Section IV, the proposed method is presented followed by Section V where the simulation results are demonstrated and comprehensively discussed. Section VI concludes main points of the paper.

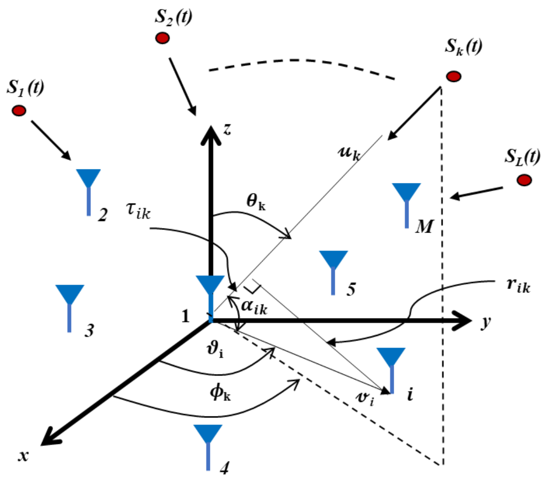

Fig. 1. AOA problem formulation with *M*-elements arbitrary array and *L* sources.

II. Wideband Signal Model and Problem Formulation

We assume that an M elements arbitrary array is used to collect information for estimating the AOAs of L ($L<M$) wideband sources as illustrated in Fig. 1.

The wideband signals arrive to the array from random directions of (θ_l, ϕ_l), l=1, 2, ⋯, L where θ_l and ϕ_l are the elevation and azimuth angles of lth signal, respectively. The wideband signals exist over the bandwidth BW between lowest frequency f_l and highest frequency f_h. The received wideband signal at mth array elements can be represented as

$$x_m(t)=\sum_{k=1}^{L}s_k\left(t-h_m\sin\theta_k\cos\phi_k\right)+n_m(t) \quad (1)$$

where $s_k(t)$ represents the kth source signal, $n_m(t)$ denotes the Additive White Gaussian Noise (AWGN) at mth channel, $h_m=(m-1)d/c$ where d and c represent the spatial separation between adjacent array elements and speed of light, respectively. To analyze the wideband signals and estimate their AOAs, they are decomposed into P narrowband signals using Fast Fourier Transform (FFT) whose output can be modelled as follows [24]:

$$\mathbf{X}_m(f_j)=\sum_{k=1}^{L}\mathbf{S}_k(f_j)e^{-j2\pi f_j h_m\sin\theta_k\cos\phi_k}+\mathbf{N}_m(f_j) \quad (2)$$

$$\mathbf{X}(f_j)=\mathbf{A}(f_j,\theta,\phi)\mathbf{S}(f_j)+\mathbf{N}(f_j) \quad (3)$$

where $\mathbf{X}(f_j)\in\mathbb{C}^{M\times 1}$ represents the frequency domain of the received signal corresponding to frequency f_j, $\mathbf{S}(f_j)\in\mathbb{C}^{L\times 1}$ is the frequency domain representation of the source signal for $f_l<f_j<f_h$ where j=1, 2, ⋯, P, $\mathbf{N}(f_j)\in\mathbb{C}^{M\times 1}$ is the AWGN at each array element for jth frequency band.

$\mathbf{A}(f_j,\theta,\phi)\in\mathbb{C}^{M\times L}$ is a steering matrix at jth frequency and it contains the steering vectors for L signals. Thus, $\mathbf{A}(f_j,\theta,\phi)$ can be represented as follows:

$$\mathbf{A}(f_j,\theta,\phi)=\left[\mathbf{a}(f_j,\theta_1,\phi_1),\ldots\mathbf{a}(f_j,\theta_L,\phi_L)\right] \quad (4)$$

where $\mathbf{a}(f_j,\theta_k,\phi_k)\in\mathbb{C}^{M\times 1}$ represents the steering vector for kth incident angle at jth frequency. In contrast to the narrowband signals, $\mathbf{a}$ is the function of both AOA and signal frequency. To drive $\mathbf{a}(f_j,\theta_k,\phi_k)$ for arbitrary array geometry shown in Fig. 1, the unit vector, $\mathbf{u}_k$, containing both θ_k and ϕ_k needs to be computed as

$$\mathbf{u}_k=\cos\phi_k\sin\theta_k\hat{a}_x+\sin\phi_k\sin\theta_k\hat{a}_y+\cos\theta_k\hat{a}_z \quad (5)$$

where $\hat{a}_x$, $\hat{a}_y$,and $\hat{a}_z$ represent the unite vectors for Cartesian coordinates. Afterwards, the second unit vector $\mathbf{v}_i$ is required to determine the spatial distance between reference element (i.e., element 1) and the ith element of the array as follows:

$$\mathbf{v}_i=r_i\cos\vartheta_i\hat{a}_x+r_i\sin\vartheta_i\hat{a}_y+z_i\hat{a}_z \quad (6)$$

where i=1, 2, ⋯, M and ϑ_i represents the angle between x-plane and the position of the ith array element. To procced, the angle between $\mathbf{u}_k$ and $\mathbf{v}_i$ for the ith sensor with respect to the reference element can be computed by

$$\begin{aligned}\alpha_{ik}&=\cos^{-1}\left(\frac{\mathbf{v}_i.\mathbf{u}_k}{\|\mathbf{v}_i\|\cdot\|\mathbf{u}_k\|}\right)\\&=\cos^{-1}\left(\frac{\sin\theta_k\cos(\phi_k-\varphi_i)+z_i\cos\theta_k}{\|\mathbf{v}_i\|\cdot\|\mathbf{u}_k\|}\right)\\&=\cos^{-1}\left(\sin\theta_k\cos(\phi_k-\varphi_i)\right)+z_i\cos\theta_k\end{aligned} \quad (7)$$

An $M\times L$ matrix can be used to represent the whole set of α_{ik} due to collecting L plane waves by M array elements as

$$\boldsymbol{\gamma}_{ik}=\begin{pmatrix}\alpha_{11}&\cdots&\alpha_{1L}\\\vdots&\ddots&\vdots\\\alpha_{M1}&\cdots&\alpha_{ML}\end{pmatrix}. \quad (8)$$

The time delay τ_{ik} corresponding to a particular angle, α_{ik}, is computed as

$$\begin{aligned}\tau_{ik}&=r\cos(\alpha_{ik})\\&=r\cos(\cos^{-1}(\sin\theta_k\cos(\phi_k-\varphi_i))+z_i\cos\theta_k)\\&=r\{\sin\theta_k\cos(\phi_k-\varphi_i))+z_i\cos\theta_k\}\end{aligned} \quad (9)$$

Similarly, the total set of τ_{ik} for L signals received by M antennas is represented as follows:

$$\mathbf{T}_{ik}=\begin{pmatrix}\tau_{11}&\cdots&\tau_{1L}\\\vdots&\ddots&\vdots\\\tau_{M1}&\cdots&\tau_{ML}\end{pmatrix}. \quad (10)$$

The angular phase difference w_{ik} can be calculated from the multiplication between τ_{ik} and propagation constant β as

$$w_{ik}=\beta\tau_{ik}=\frac{2\pi}{\lambda}\tau_{ik}, \quad (11)$$

where λ is the signal wavelength. The total phase differences corresponding to $\mathbf{T}_{ik}$ are presented by

$$\mathbf{\Xi}_{ik} = \begin{pmatrix} w_{11} & \cdots & w_{1L} \\ \vdots & \ddots & \vdots \\ w_{M1} & \cdots & w_{ML} \end{pmatrix}. \tag{12}$$

w_{ik} contains information about elevation and azimuth angles. Therefore, the $M\times1$ steering vector at jth frequency band for kth signal arrived to the arbitrary array shown in Fig. 1 can be modelled as follows:

$$\mathbf{a}(f_j,\theta_k,\phi_k) = \left[e^{-jf_j w_{1k}}, e^{-jf_j w_{2k}}, \cdots, e^{-jf_j w_{Mk}}\right]^T. \tag{13}$$

This work considers 1D AOA estimation. Henceforward, we represent $\mathbf{A}(f_j,\theta,\phi)$ and $\mathbf{a}(f_j,\theta_k,\phi_k)$ as $\mathbf{A}_j(\theta)$ and $\mathbf{a}_j(\theta_k)$, respectively. The CM of the received data is computed by

$$\begin{aligned} \mathbf{R}_{xx}(f_j) &= E\left\{\mathbf{X}(f_j)\mathbf{X}^H(f_j)\right\} \\ \mathbf{R}_{xx}(f_j) &= \mathbf{A}_j(\theta)\mathbf{R}_{ss}(f_j)\mathbf{A}_j^H(\theta) + \sigma^2(f_j)\mathbf{I}_M \end{aligned} \tag{14}$$

where $E\{\cdot\}$ and $(\cdot)^H$ denote the statistical expectation and conjugate transpose operator, respectively. $\mathbf{R}_{ss}(f_j)$ is the signal CM at jth frequency band. $\sigma^2(f_j)$ represents the variance of the noise which is uncorrelated with the signals and $\mathbf{I}_M$ is the $M\times M$ identity matrix. Practically, $\mathbf{R}_{xx}(f_j)$ is estimated over finite N snapshots as follows:

$$\mathbf{R}_{xx}(f_j) = \frac{1}{N}\sum_{i=1}^{N}\mathbf{X}_i(f_j)\mathbf{X}_i^H(f_j). \tag{15}$$

III. TOPS Based AOA Estimation Algorithms

When the wideband sources are totally non-correlated, the EVD technique is usually applied to extract SS, $\mathbf{F}_j$, and NS, $\mathbf{W}_j$, from the $\mathbf{R}_{xx}(f_j)$. These subspaces can be represented by

$$\mathbf{F}_j = \left[\mathbf{q}_{j,1}, \mathbf{q}_{j,2}, \dots, \mathbf{q}_{j,L}\right], \tag{16}$$

$$\mathbf{W}_j = \left[\mathbf{q}_{j,L+1}, \mathbf{q}_{j,L+2}, \dots \mathbf{q}_{j,M}\right], \tag{17}$$

where $\mathbf{q}_{j,1}, \mathbf{q}_{j,2}, \cdots, \mathbf{q}_{j,M}$ denote the eigenvectors of $\mathbf{R}_{xx}(f_j)$ sorted in descending order with respect to their corresponding eigenvalues as follows:

$$\lambda_{j,1} \ge \lambda_{j,2} \ge \cdots \lambda_{j,L} > \lambda_{j,L+1} = \cdots = \lambda_{j,M} = \sigma^2. \tag{18}$$

After formulating $\mathbf{F}_j$ and $\mathbf{W}_j$, TOPS based algorithms select a certain frequency band known as reference frequency for SS. To explore multiple frequency components, a transformation matrix is used to transfer the SS for the reference frequency into other frequencies. Finally, the orthogonality between the transferred SS and the NSs is tested at each hypothesized angle to estimate the AOA of the wideband sources.

A. Standard TOPS Algorithm

Assume that ω_i is selected as a reference frequency and the SS at this band is transferred into other bands by

$$\mathbf{U}_j(\theta) = \mathbf{\Psi}\left(\Delta\omega_j, \theta\right)\mathbf{F}_i, \quad i \ne j \tag{19}$$

where $\mathbf{U}_j(\theta)$ is the transferred SS from ω_i to ω_j, $\mathbf{F}_i$ is the SS at reference frequency, $\Delta\omega_j = \omega_j - \omega_i$, and $\mathbf{\Psi}(\Delta\omega_j, \theta)$ is a full rank and diagonal transformation matrix, which transfers $\mathbf{F}_i$ to other frequencies, and defined as follows:

$$\mathbf{\Psi}(\Delta\omega_j, \theta)_{M\times M} = \mathrm{diag}\{\mathbf{a}(\Delta\omega_j, \theta)\}. \tag{20}$$

The mth element on the diagonal of $\mathbf{\Psi}(\Delta\omega_j, \theta)$ is as follows:

$$\left[\mathbf{\Psi}(\Delta\omega_j, \theta)\right]_{m\times m} = \exp\left(-j\omega_j\frac{md}{c}\sin(\theta)\right). \tag{21}$$

We apply this transformation at each hypothesized search angle φ to test the orthogonality between the transferred SS and NSs over all the scanned ranges as:

$$\mathbf{U}_j(\varphi) = \mathbf{\Psi}(\Delta\omega_j, \varphi)\mathbf{F}_i. \quad i \ne j \tag{22}$$

Afterwards, we define an $L\times(P-1)(M-L)$ matrix, $\mathbf{D}(\varphi)$ as follows:

$$\mathbf{D}(\varphi) = \left[\mathbf{U}_2^H\mathbf{W}_2 \;\; \mathbf{U}_3^H\mathbf{W}_3 \cdots \mathbf{U}_P^H\mathbf{W}_P\right]. \tag{23}$$

The estimator matrix $\mathbf{D}(\varphi)$ becomes rank-deficient (i.e., losses its rank) if φ is equal to the true angle of the incident signal. The AOA estimation accuracy directly related to the accuracy of the CM estimation. The values of N and SNR (which are not controllable by the array processor) determine the precision of the CM estimation. Some of the errors within $\mathbf{D}(\varphi)$ can be reduced by applying subspace projection as follows:

$$\mathbf{P}_j(\varphi) = \mathbf{I}_M - \left(\mathbf{a}_j^H(\varphi)\mathbf{a}_j(\varphi)\right)^{-1}\mathbf{a}_j(\varphi)\mathbf{a}_j^H(\varphi) \tag{24}$$

where $\mathbf{P}_j(\varphi)$is the projection onto the null space of $\mathbf{a}_j(\vartheta)$. The transformed signals subspace can be updated by

$$\mathbf{U}_j' = \mathbf{P}_j(\varphi)\mathbf{U}_j(\varphi). \tag{25}$$

The estimator matrix $\mathbf{D}(\varphi)$ is modified as

$$\begin{aligned} \mathbf{D}'(\varphi) &= \left[\mathbf{U}_2'^H(\varphi)\mathbf{W}_2 \;\; \mathbf{U}_3'^H(\varphi)\mathbf{W}_3 \cdots \mathbf{U}_P'^H(\varphi)\mathbf{W}_P\right] \\ &= \left[\mathbf{U}_2^H(\varphi)\mathbf{P}_2^H(\varphi)\mathbf{W}_2 \cdots \mathbf{U}_P^H(\varphi)\mathbf{P}_P^H(\varphi)\mathbf{W}_P\right]. \end{aligned} \tag{26}$$

Better estimation accuracy can be obtained by using $\mathbf{D}'(\varphi)$ rather than $\mathbf{D}(\varphi)$. This is because the errors produced due to interfering some SS component into $\mathbf{W}_j$ is removed by the projection matrix $\mathbf{P}_j(\varphi)$. Thus, the spatial spectrum of the standard TOPS algorithm is generated as follows:

$$Y_{\mathrm{TOPS}}(\varphi) = \arg\max\left(\frac{1}{\rho_{\min}'(\varphi)}\right), \tag{27}$$

where $\rho_{\min}'(\varphi)$ denotes the smallest singular value of $\mathbf{D}'(\varphi)$.

B. Squared TOPS (SQ-TOPS)

Using the transferred SS in (25) and NS $\mathbf{W}_j$ the SQ-TOPS establishes a squared evaluation matrix $\mathbf{Z}(\varphi)$ as follows:

$$\mathbf{Z}(\varphi) = [\mathbf{U}_j'^H(\varphi)\mathbf{W}_j\mathbf{W}_j^H\mathbf{U}_j'(\varphi)], \text{ for } 2 \le j \le P \quad (28)$$

Similar to (27), the SQ-TOPS spectrum is generated by

$$Y_{\text{SQ-TOPS}}(\varphi) = \arg\max\left(\frac{1}{\rho_{Z,\min}(\varphi)}\right), \quad (29)$$

where $\rho_{Z,\min}(\varphi)$ is the minimum singular value of $\mathbf{Z}(\varphi)$. The sensitivity to detect rank-deficiency in $\mathbf{Z}(\varphi)$ is improved compared to (27) because all the elements (i.e., rows and columns) of $\mathbf{Z}(\varphi)$ have to be close to zero when φ equals one of the true AOAs. This will enhance estimation performance of SQ-TOPS in comparison to the standard TOPS method. This modification, however, adds more complexity to the standard TOPS algorithm and it is unable to resolve the false peaks problem in the spatial spectrum.

C. Weighted Squared TOPS (WS-TOPS)

WS-TOPS algorithm conducts two enhancements to the SQ-TOPS method. The first improvement removes the false peaks through adding a new term to the evaluation matrix $\mathbf{Z}(\varphi)$ in (28) as follows:

$$\begin{aligned}\mathbf{H}_j(\varphi) &= \mathbf{U}_j'^H(\varphi)\mathbf{W}_j\mathbf{W}_j^H\mathbf{U}_j'(\varphi) + \\ &\left\{\mathbf{a}_j^H(\varphi)\mathbf{W}_j\mathbf{W}_j^H\mathbf{a}_j(\varphi)\right\}\frac{1}{M}\mathbf{I}_L,\end{aligned} \quad (30)$$

$$\mathbf{Z}'(\varphi) = \left\{\mathbf{H}_j\right\}, \text{ for } 2 \le j \le P \quad (31)$$

where $\mathbf{I}_L$ is an $L \times L$ identity matrix. The estimated AOAs correspond to the smallest singular values of $\mathbf{Z}'(\varphi)$. In the second enhancement, a new weighting factor, ε_i, was added to the spatial spectrum equation in (29) and defined as

$$\varepsilon_i = \frac{\lambda_{s,\min}}{\lambda_{n,\max}}, \quad (32)$$

where $\lambda_{s,\min}$ and $\lambda_{n,\max}$ are the minimum signal eigenvalue and maximum noise eigenvalue, respectively. This weighting factor may seriously affect the estimation accuracy when the frequency bands are too noisy. To solve this, the frequency bands with a weighting factor ε_i greater than a pre-defined threshold ε_{th}, are only used. These two modifications are combined and the spatial spectrum of the WS-TOPS is generated based on the following formula:

$$Y_{\text{WS-TOPS}}(\varphi) = \arg\max\left(\frac{P'}{\frac{1}{P}\sum_{i=1}^{P}\varepsilon_i\rho_{\mathbf{Z}_i',\min}(\varphi)}\right), \quad (33)$$

where P' is the number of frequency bands with $\varepsilon_i > \varepsilon_{\text{th}}$. These two steps improve estimation accuracy and removes false peaks. However, these improvements come at the cost of higher computational complexity. Meaning that the computational cost of the WS-TOPS is considerably higher than both standard TOPS and SQ-TOPS algorithms. In the following section, we propose a new SQ-TOPS based AOA estimation that outclasses the presented methods in terms of not only estimation accuracy, but also computational complexity.

IV. Proposed Method

The proposed PMS-TOPS algorithm applies two key modifications to the SQ-TOPS algorithm. First, it avoids the complex EVD technique through constructing a low-complex PM based on a novel CM sampling technique. Thus, in the proposed method the extraction of $\mathbf{W}_j$ is totally avoided. This modification curtains the overall complexity of the algorithm, makes it less sensitive to the correlated sources, and improves estimation accuracy at low and mid SNR regions. Second, PMS-TOPS establishes a new squared orthogonality evaluation matrix between the transferred SS and the newly created PM at each frequency band. This step will diminish the false peaks generated primarily due to projecting the NS to the signal null-space [26] in the traditional TOPS-based methods. These two steps are detailed below.

A. Replacing EVD with Direct PM Construction via CM Subsampling

In AOA estimation problem, a PM $\mathbf{V}$ is constructed, whose null space equals to the SS. It is easy to show that the solution of $\mathbf{V}$ is as follows:

$$\mathbf{V} = \mathbf{I}_M - \mathbf{Q}\left(\mathbf{Q}^H\mathbf{Q}\right)^{-1}\mathbf{Q}^H, \quad (34)$$

where $\mathbf{Q}$ is an $M \times L$ matrix which its columns span the same space as SS. When the sources are independent, L columns from the CM can be extracted to obtain the sampled matrix $\mathbf{Q}$ [25]. From this perspective, we construct the PM based on the CM columns. Different sampling methodologies proposed in literature to formulate sampled matrix $\mathbf{Q}$ from the direct extraction of CM columns [25], [27], [28]. However, none of the existing sampling methodologies takes the correlations between the selected columns into consideration. This will have negative effect on the PM construction and hence on AOA estimations. To extract as much non-redundant information about the incident signals as possible, we propose to select the L independent columns from the CM to form the matrix sketch $\mathbf{Q}$. In such case, the PM is constructed based on the L columns of the CM that are least-dependent. In addition to reducing the complexity, this modification makes the AOA estimation method to be less affected by the correlated sources due to removing the dependency with steering vector [27]. The observed CM in (15) can be re-written as follows:

$$\mathbf{R}_{xx}(f_j)=\begin{pmatrix} r_{11}(f_j) & \cdots & r_{1M}(f_j) \\ \vdots & \ddots & \vdots \\ r_{M1}(f_j) & \cdots & r_{MM}(f_j) \end{pmatrix}. \tag{35}$$

The fundamental question now is which L columns need to be used out of M columns to construct the sketch matrix $\mathbf{Q}$. The recently developed method in [28] selects L columns randomly. However, this is not an optimum selection as the dependency between the selected columns has been ignored. Additionally, in case of correlated sources, $\mathbf{R}_{xx}(f_j)$ becomes rank-deficient and some columns of $\mathbf{Q}$, eventually become redundant. Alternatively, we select L columns at jth frequency band to construct matrix $\mathbf{Q}(f_j)$ as follows:

$$\mathbf{Q}(f_j)=\begin{Bmatrix} r_{1b}(f_j) & \cdots & r_{1b}(f_j) \\ \vdots & \ddots & \vdots \\ r_{Mb}(f_j) & \cdots & r_{Mb}(f_j) \end{Bmatrix}, \tag{36}$$

where $b=b_k$ given that b_k is a non-repeated random variable within the set and defined as

$$b=\mathbb{Z}_M=\{1,2,\ldots,M\},\ \text{for } 1<k<L$$

It is well known that the off-diagonal components of the CM represent the correlation between signals collected from different array elements. To extract more non-identical information about the incident signals, we select the value of b such that the corresponding columns contain least correlation between signals collected from the different array elements. This can be accomplished by selecting columns with minimum norm, which directly implies that the correlation coefficient within that column is minimum, as illustrated in Fig. 2.

Selecting columns based on the presented method results minimum dependency between adjacent columns within the sampled matrix $\mathbf{Q}(f_j)\in\mathbb{C}^{M\times L}$. Therefore, $\mathbf{Q}(f_j)$ provides a good representation of the general trend of the CM and retains more valuable information about the wideband source directions. Hence, we construct the PM at jth frequency band, $\mathbf{V}(f_j)$, by projecting onto the null-space of sampled matrix $\mathbf{Q}(f_j)$ as follows:

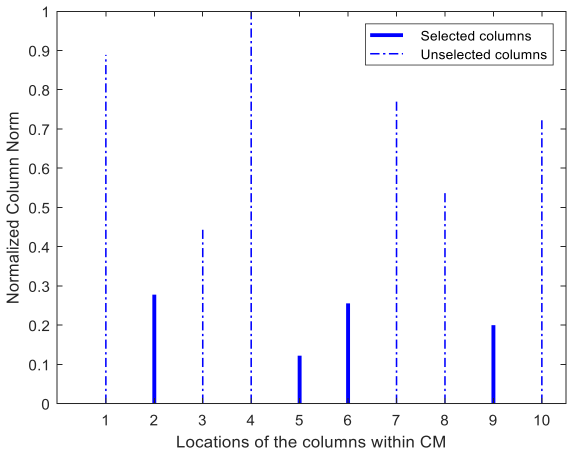

Fig. 2. Conceptual illustration of selecting\extracting four columns (L=4) from the CM $\text{CM}\in\mathbb{C}^{10\times10}$ using the new sampling methodology to form the sampled matrix $\mathbf{Q}(f_j)$ required for PM construction.

$$\mathbf{V}(f_j)=\mathbf{I}_M-\mathbf{Q}(f_j)\left(\mathbf{Q}^H(f_j)\mathbf{Q}(f_j)\right)^{-1}\mathbf{Q}^H(f_j). \tag{37}$$

It is stated in [27] that the dimension of $\mathbf{V}(f_j)$ can be reduced from $M\times M$ to $M\times L$ without sacrificing estimation accuracy.

To prevent high-complexity of computing evaluation matrix, we apply the following dimension reduction to $\mathbf{V}(f_j)$:

$$\mathbf{V}(f_j)=\mathbf{V}(f_j)\times\mathbf{I}_{M\times L}, \tag{38}$$

where $\mathbf{I}_{M\times L}$ is defined as follows:

$$\mathbf{I}_{M\times L}=\begin{bmatrix} 1 & 0 & \cdots & 0 \\ 0 & 1 & \cdots & 0 \\ \vdots & \vdots & \cdots & \vdots \\ 0 & 0 & \cdots & 1 \\ 0 & 0 & \ddots & 0 \\ 0 & 0 & \cdots & 0 \end{bmatrix}$$

To what follows, $\mathbf{V}(f_j)\in\mathbb{C}^{M\times L}$ is represented as $\mathbf{V}_j$.

B. A New Squared Evaluation Matrix

Following the guidance of [23], [29], one of the appropriate choices of reference frequency is central frequency. Therefore, in this work center frequency is selected for the SS. A new transferred SS $\mathbf{H}_j(\varphi)$ is formed by

$$\mathbf{H}_j(\varphi)=\boldsymbol{\Psi}(\Delta\omega_j,\varphi)\mathbf{F}_c\,, \tag{39}$$

where $\Delta\omega_j=\omega_j-\omega_c$, for $\omega_j\neq\omega_c$, ω_c is the central frequency, and $\mathbf{F}_c$ is the SS at ω_c. Then, similar to the TOPS based methods, we apply subspace projection as follows:

$$\mathbf{H}'_j(\varphi)=\mathbf{P}_j(\varphi)\mathbf{H}_j(\varphi)\,. \tag{40}$$

As mentioned above, the TOPS, SQ-TOPS, and WS-TOPS algorithms conduct the orthogonality test between transferred SS and NSs. So, the jth partition of their evaluation matrices can be expanded as

$$\mathbf{U}'^H_j(\varphi)\mathbf{W}_j=\mathbf{U}^H_j\mathbf{P}_j(\varphi)\mathbf{W}_j\,. \tag{41}$$

It is shown in [26] that the dot-product between $\mathbf{W}_j$ and $\mathbf{P}_j(\varphi)$, which is termed as signal null-space, reinforces the noise components and contributes to the reasons of generating the false peaks in the spectrum of the TOPS-based algorithms. It is found that using an efficient PM instead of the NS in (28) will reduce the effect of this problem and eventually minimizes false peaks. This has motivated our second modification; employing orthogonality between transferred SS and the newly created PM rather than NS. Thus, the proposed algorithm modifies the contents of $\mathbf{Z}_i(\varphi)$ and employs a new squared orthogonality evaluation matrix for each AOA assumption as follows:

$$\mathbf{G}(\varphi)=\left[\mathbf{H}'^H_j(\varphi)\mathbf{V}_j\mathbf{V}^H_j\mathbf{H}'_j(\varphi)\right],\ \text{for } 2\le j\le P \tag{42}$$

when $\varphi=\theta_l$ for $1\le l\le L$, the following equality yields.

$$\mathbf{H}_j'^H(\varphi)\mathbf{V}_j\mathbf{V}_j^H\mathbf{H}_j'(\varphi) \approx 0. \qquad (43)$$

The proof of (43) is straightforward as follows: Let us assume that one of the null spaces of the PM is spanned by the bases of matrix $\mathbf{E}_j \in \mathbb{C}^{M\times L} = [\mathbf{e}_{j1}\ \mathbf{e}_{j2}\ \cdots\ \mathbf{e}_{jL}]$. From linear algebra, if $\mathbf{A} \in \text{Null}(\mathbf{B})$, then $\mathbf{A} \perp \text{Col}(\mathbf{B})$. From this fact, the following equality yields.

$$\mathbf{E}_j^H\mathbf{V}_j = \left[\mathbf{e}_{j1}^H\mathbf{v}_{j1}\quad \mathbf{e}_{j2}^H\mathbf{v}_{j2}\quad \cdots\quad \mathbf{e}_{jL}^H\mathbf{v}_{jL}\right] \approx 0. \qquad (44)$$

By definition the SS $\mathbf{H}_j$ is in the null-space of $\mathbf{V}_j$, that is $\mathbf{H}_j \in \text{Null}(\mathbf{V}_j)$, and so does $\mathbf{H}_j'$ Therefore, we can conclude that the following equation is satisfied:

$$\mathbf{H}_j'^H(\varphi)\mathbf{V}_j \approx 0, \qquad (45)$$

which justifies that the orthogonality between the transferred SS and the newly created PM is preserved.

Finally, the spatial spectrum of the proposed algorithm is generated as follows:

$$Y_{\text{proposed}}(\varphi) = \arg\max\left(\frac{1}{\rho_{\mathbf{G},\min}(\varphi)}\right), \qquad (46)$$

where $\rho_{\mathbf{G},\min}(\varphi)$ represents the minimum singular values of $\mathbf{G}_i(\varphi)$. The following steps summarize proposed method:

- Step 1: Divide the output of the antenna array into multiple identical sized blocks where the number of samples in each block equals to the DFT points.
- Step 2: Apply temporal DFT to each block and compute $\mathbf{R}_{xx}(f_j)$ using (15).
- Step 3: Construct the PM $\mathbf{V}_j$ based on the presented methodology using (36), (37), and (38).
- Step 4: Apply one EVD to extract the SS at reference frequency and construct $\mathbf{H}_j'(\varphi)$ using (40).
- Step 5: Establish a new squared orthogonality evaluation matrix $\mathbf{G}(\varphi)$ using (42).
- Step 6: Estimate the AOAs of wideband sources using (46).

C. *The Computational Complexity Analysis*

Low complexity is of significant practical importance since limited power applications, such as IoT and UAV, call for low-complex AOA estimation algorithms particularly when array size is large. The overall complexity of the TOPS based algorithms can be divided into three main stages. First, extracting the subspaces from the CM, we called subspaces acquisition stage. Second, computation of the evaluation matrix $(\mathbf{D},\ \mathbf{Z},\ \mathbf{Z}',\text{ and }\mathbf{G})$. Third, spectrum construction through calculation of minimum singular values of $\mathbf{D},\mathbf{Z},\mathbf{Z}',$ and $\mathbf{G}$

The complexity of subspaces acquisition dominants the overall computational burden of the TOPS based methods. This is because the complexity of EVD applied to an $M\times M$ matrix is $O(M^3)$ [30] and this process has to be repeated for P frequency bins to extract $\mathbf{W}_j$ where $1 \le j \le P$. However, the proposed method needs only one EVD to extract SS at $\mathbf{F}_c$ and the rest $P-1$ EVDs are replaced by the low complex PM construction ($\mathbf{V}_j$) (which requires $O(M^2L)$ arithmetic operations [25], [27]. Further, the proposed method has comparably lower complexity in the second stage particularly when $M >> L$. This is because the dimensions of $\mathbf{W}_j$ and $\mathbf{V}_j$, respectively, are $M\times(M-L)$ and $M\times L$. Therefore, the computation of matrix $\mathbf{G}$ which is the function of the PM $\mathbf{V}_j$ needs less operations compared to matrices $\mathbf{D}$, $\mathbf{Z}$, and $\mathbf{Z}'$ which are the functions of $\mathbf{W}_j$. Besides, the WS-TOPS algorithm needs extra $O(2ML(M-L)+L^2(M-L))$ operations to calculate the new term in (30). All the algorithms have comparable complexity in the third stage except WS-TOPS that needs to repeat SVD P' times. The overall computational complexities for all the presented algorithms are listed in Table I.

As the signal processing costs for all algorithms mainly depend on the array size, a numerical example of the computational complexity versus different values of M for all the presented algorithms is conduced and illustrated in Fig. 3. Due to the need for P' extra signal processing, computational cost of the WS-TOPS is higher than all the other methods. It is also observable that SQ-TOPS needs higher arithmetic operations compared to the standard TOPS algorithm. This is due to performing squared test of orthogonality in matrix $\mathbf{Z}$. Importantly, the figure clearly justifies that the proposed algorithm has much less complexity among its rival methods. The gap between the complexity of the proposed method and its counterparts become even wider as the physical array dimension increases. This low complexity of the suggested method, in turn, will have a positive impact on its execution speed and, consequently, enables it to localize sources with relatively minimum amount of time as will be shown in the following section.

TABLE I: COMPUTATIONAL COMPLEXITY COMPARISON

Algorithm	Over all signal processing cost		
	Subspace acquisition	Computation of $\mathbf{D},\mathbf{Z},\mathbf{Z}',\text{and}\,\mathbf{G}$	SVD of $\mathbf{D},\mathbf{Z},\mathbf{Z}',\text{and}\,\mathbf{G}$
TOPS	$O(M^3(P))$	$+O\left(ML(M-L)(P-1)\right)$	$+O[L^2(M-L)(P-1)]$
SQ-TOPS	$O(M^3(P))$	$+O\{[2ML(M-L)+L^2(M-L)](p-1)\}$	$+O[L^3(P-1)]$
WS-TOPS	$O(M^3(P))$	$+O\left(2ML(M-L)+L^2(M-L)+\{2ML(M-L)+L^2(M-L)\}(P-1)P'\right)$	$+O\left(L^3(P-1)P'\right)$
Proposed	$O(M^3+M^2L(P-1))$	$+O[(2ML^2+L^3)(P-1)]$	$+O[L^3(P-1)]$

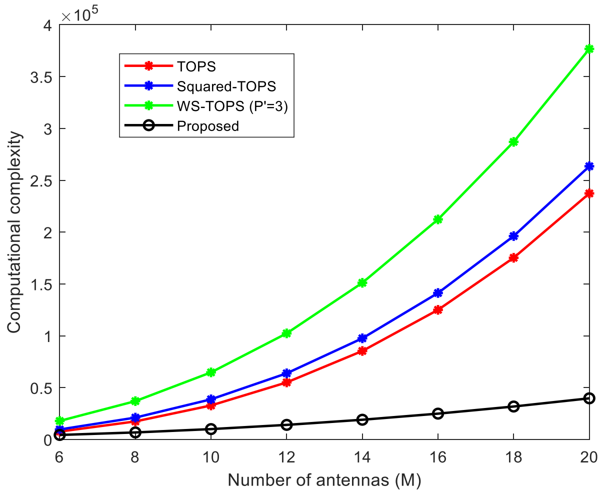

Fig. 3. Computational complexity versus the number of antennas within the array for the proposed algorithm, TOPS, SQ-TOPS, and WS-TOPS algorithms, $L=3, P=20$.

V. Simulation Results and Discussion

In this section, we evaluate the performance of the proposed algorithm by comparing it to the well-known TOPS based AOA estimation methods from various perspectives. In all the simulation scenarios, the data are generated from unit-power complex Gaussian process with zero mean. All the signals have identical frequency within $f_l = 200$ MHz and $f_h = 400$ MHz.

The bandwidth of all the wideband signals BW $= f_h - f_l = 400 - 200$ MHz and the f_c and sampling frequency f_s, respectively, are 300 MHz and twice the signal's bandwidth. FFT is applied to decompose the received wideband signal into $P = 20$ narrowband signals each with $200/20 = 10$ MHz bandwidth. To avoid aliasing, the distance between adjacent array element d is set to be $\lambda/2$ where λ is a wavelength corresponding to the highest frequency of the received signals. The hypothesized search angle is used over the grid of –90° to 90° with the 0.5° step size. As the measure of performance, average root mean square error (ARMSE) and probability of successful detections (PSDs) are computed for all the evaluated algorithms as follows:

$$\text{ARMSE}=\frac{1}{K}\sum_{i=1}^{K}\sqrt{\frac{1}{L}\left[\left(\theta_k-\hat{\theta}_k\right)^2\right]}, \tag{47}$$

$$\text{PSD(AOA)} = \frac{\sum_{i=1}^{K}\Omega_i}{KL}, \tag{48}$$

where K represents the number of Monte Carlo iterations, θ_k and $\hat{\theta}_k$ are true and estimated AOA, respectively. Ω_i denotes the number of successful detections at ith iteration.

A. Spatial Spectrum: Numerical Example

The spatial spectrum illustrates the AOA estimation results for each hypothesis angle where the peaks indicate estimated angles. This section illustrates the effectiveness of the proposed method to remove the false peaks appearing in the spatial spectrum of the TOPS, and SQ-TOPS methods. We assume that three wideband signals with the properties mentioned above impinging on the seven-elements receiver array (M=7) at –33°, 0°, and 33° elevation angles. In this scenario, the SNR and number of snapshots (N) are 10 dB and 100, respectively. The spatial spectrum of the proposed method is compared with those for the TOPS, SQ-TOPS and WS-TOPS algorithms in Fig. 4. The figure shows that all methods have detected all three AOAs but with different resolutions.

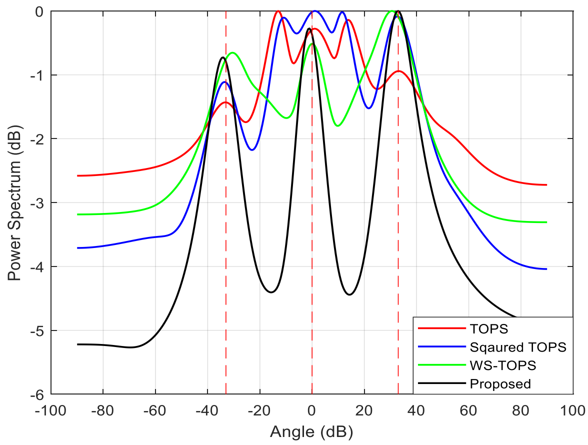

Fig. 4. Illustration of spatial spectrums of the TOPS, SQ-TOPS, WS-TOPS algorithms and proposed method.

It is observable that TOPS and SQ-TOPS methods share a common problem which is the high-power false peaks at wrong directions. Noticeably, the power of the false peaks in the standard TOPS algorithm is higher than the power of the true peaks. These side fluctuations mislead the estimator to detect actual AOAs and, eventually, results false estimation. On the other side, the proposed algorithm along with WS-TOPS do not show any fluctuations at wrong angles. However, the WS-TOPS obtained this improvement at the cost of adding more computational cost. It is worth mentioning that, in addition to its low complexity, the proposed method is superior and shows best resolution and highest noise immunity among the compared methods.

B. Performance Comparison Based on SNR Variations

Due to multipath fading phenomenon, high SNR may not be always available and its values usually fluctuates. Thus, it is particularly important for the estimator to perform well within various SNR ranges. In this experiment, the AMRSE and PSD of the proposed algorithm are computed and compared to those of other methods with different SNR levels. The SNR is postulated to vary from 0 dB to 20 dB with 5 dB increments. We apply the same simulation parameters used in Section V-A except M=8. For each SNR value, one-hundred Monte Carlo simulations (K=100) are applied to all the algorithms independently and their estimation errors and PSDs are calculated and plotted as shown in Fig. 5 and Fig. 6, respectively.

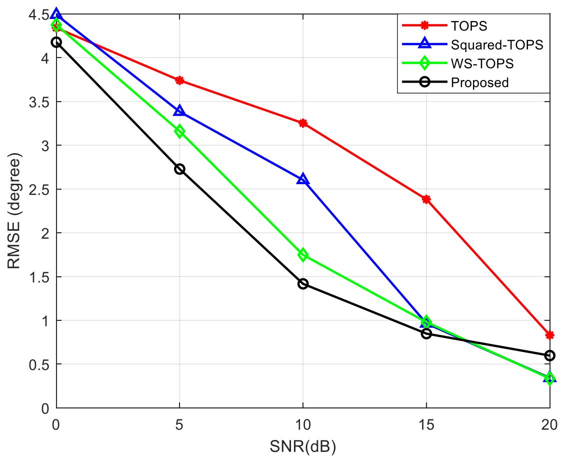

Fig. 5. ARMSE vs SNR for the three incident angles shown in Fig. 4.

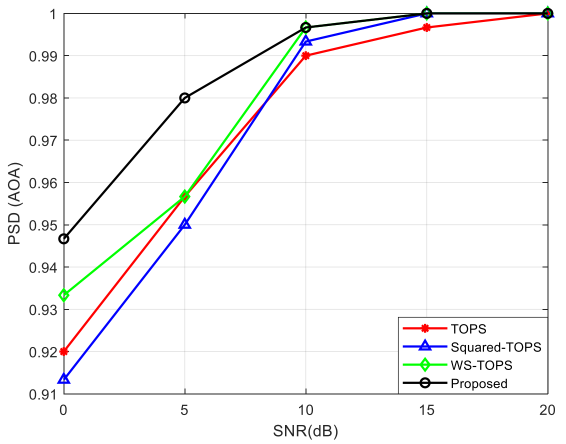

Fig. 6. PSDs vs SNR for the three incident angles shown in Fig. 4.

Fig. 5 shows that remarkable advantages in terms of low ARMSE has been achieved over SNR range from 0 dB to 16 dB due to applying the proposed method compared to the other methods. Beyond 16 dB, SQ-TOPS and WS-TOPS shows lower estimation errors. It is worth mentioning that the SQ-TOPS and WS-TOPS reduces estimation error at the cost of higher computational complexity. Nevertheless, Fig. 6 depicts that the newly applied method outperformed its counterparts in terms of highest PSDs over 0 to 10 dB SNR ranges. From 15 dB, WS-TOPS shows the same performance as the suggested method. It is observable that at high SNR (20 dB), the PSDs of the all methods become identical and reach to their highest values. This high performance of the proposed method comes along with considerably lower complexity in comparison to the compared methods.

C. Performance Comparison Based on Correlation Levels between Incident Signals

The TOPS based algorithms assume that incident signals are independent and the measured CM has a full rank property. To deal with correlated signals, they need a pre-processing step [23] which adds extra cost to the algorithm's procedure. Therefore, it is particularly important to deal with coherent sources intelligently without adding extra-complexity. In this section, the accuracy of the proposed algorithm is compared to its competitors in cases where the incident wideband signals are slightly, moderately, and strongly correlated. In this simulation, three wideband signals incident to the receiver array (M=8) at –33°, 0°, and 33° angles, respectively. It is assumed that the first signal is independent and the last two signals are correlated with each other but uncorrelated with the first one. That is to say, there are only two signals and the last one at 33° resulted from the reflection of the second one. We consider three correlation levels $CC_{2,3}$=[0.1, 0.5, 0.99], where $CC_{2,3}$ is the correlation coefficient between the second and third signals. The SNR is set to be 10 dB and we conduct the same number of Monte Carlo iterations as Section V-B for each value of $CC_{2,3}$. The ARMSE and PSDs for all the algorithms are computed independently as shown in Fig. 7 and Fig. 8, respectively.

From Fig. 7, it is shown that standard TOPS algorithm has highest estimation errors in all the correlation cases followed by the SQ-TOPS, WS-TOPS, and then the proposed method, respectively. According to the Fig. 8, when $CC_{2,3}$=0.1 the PSD of the SQ-TOPS and WS-TOPS are almost the same and higher than that for the TOPS algorithm. Furthermore, the performance of SQ-TOPS and WS-TOPS degrades more than original TOPS when signals are moderately ($CC_{2,3}$=0.5) and strongly ($CC_{2,3}$=0.99) correlated.

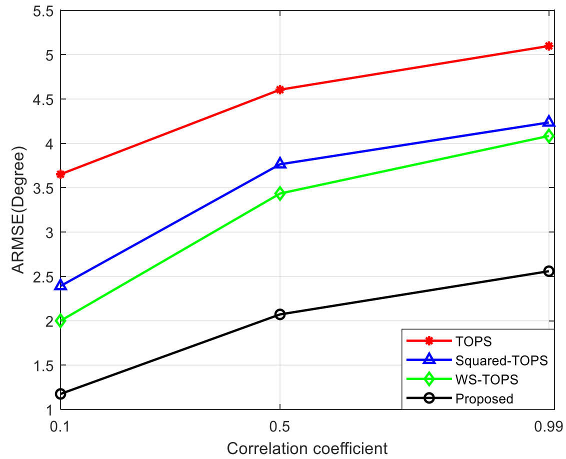

Fig. 7. ARMSE of the proposed and other algorithms where the two signals at 0° and 33° angles are slightly, moderately, and strongly correlated.

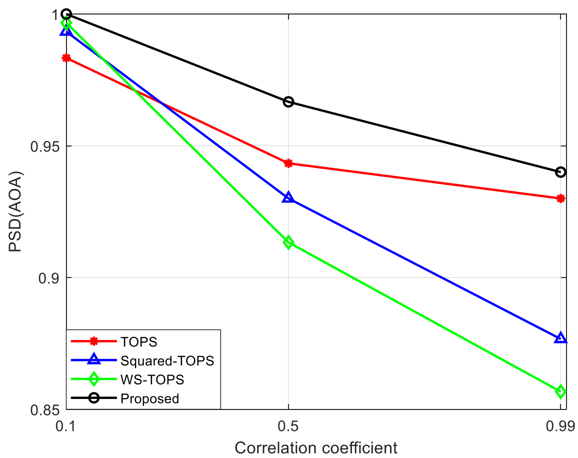

Fig. 8. PSDs of the proposed and other algorithms where the two signals at 0° and 33° angles are slightly, moderately, and strongly correlated.

From both figures, the proposed method attains best estimation accuracy (i.e., minimum ARMSE and highest PSDs) at all the correlation levels where the TOPS, SQ-TOPS, and WS-TOPS methods experience significant vulnerability. This is because subspace acquisition using EVD are more sensitive to the correlated sources due to decreasing the CM rank from 1 to $M-1$ depending on the correlation levels. On the other side, the proposed method partially solves this problem by replacing subspaces extraction to a novel PM constructed based on a new sampling methodology that removes the dependency with the steering vector. Consequently, the proposed AOA estimation algorithm shows more robustness and less sensitivity to the correlated signals.

D. Execution Time Comparison

In this section, the execution time of the proposed method is compared with that for TOPS, SQ-TOPS and WS-TOPS algorithms in an identical situation. The property of the PC used for computation is Intel CPU i3-2330M (2.20GHz), 4GB Installed RAM. The program is run using MATLAB R2021a. The exact values of the consumed time for each algorithm could be different from the values presented below depending on the machine capability for computation, however, the relative execution time differences between the algorithms must remain unchanged.

1) EVD and PM Construction

We firstly compare the time needed to extract subspaces using EVD and the required time to construct the PM based on the proposed technique. To achieve this, we apply one-hundred Monte Carlo iterations (K=100) to extract subspaces using EVD and construct PMs using the proposed sampling approach. For each iteration, the execution time is calculated for each methodology and then plotted as a cumulative distribution function (CDF). As illustrated in Fig. 9, EVD applied to CM consumes significantly more time than the PM constructions based on the presented technique. This, in turn, makes the proposed AOA estimation method much faster than its rival algorithms.

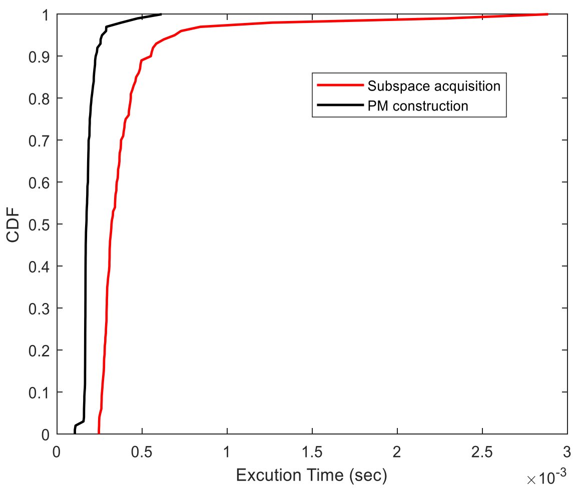

Fig. 9. CDF of execution time required for subspace acquisition using EVD and PM construction based on the new sampling technique adapted in the proposed method, $L=3, M=10, N=100$.

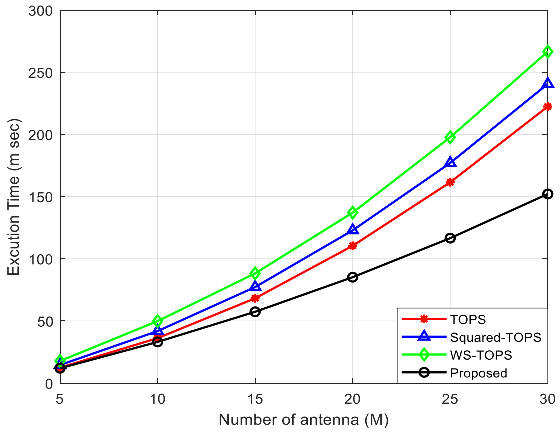

Fig. 10. Execution time versus number of array elements, $L=3$.

2) Overall Execution Time Versus the Number of Array Elements

The complexity of all the presented algorithms is mainly driven by the array size as shown in Table1. Therefore, it is reasonable to observe the speed of these algorithms with different values of M. The overall execution times for all the algorithms are computed against different array sizes, that is M=[5 10 15 20 25 30] as shown in Fig. 10. The figure depicts that the proposed algorithm is the fastest method among the compared algorithms and needs least-time to converge. Whereas, the WS-TOPS is the slowest method and has relatively highest execution time followed by the SQ-TOPS and TOPS methods, respectively.

The reason for that high speed of the proposed algorithm is that it does not need EVD technique adapted in the compared algorithms. Noticeably, the execution time differences between proposed and its counterpart methods becomes even wider as the array size increases.

3) Overall Execution Time Versus Simulation Rounds

To further confirm the speed of the suggested method, all the simulation parameters including L=3 and M=10 are fixed then the program is run for all the algorithms independently over two-hundred simulation rounds (K=200). For each simulation round, the execution time for all the algorithms is recorded and the obtained results are illustrated in Fig. 11. The figure clearly shows that the proposed algorithm outclasses other algorithms with lowest consumed time for all the simulation rounds.

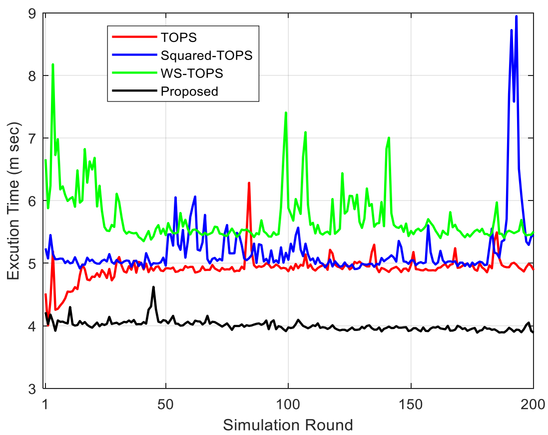

Fig. 11. Execution Time for 200 simulation rounds.

VI. Conclusion

The TOPS, SQ-TOPS and WS-TOPS algorithms share a common limitation which is the high complexity resulted from applying EVD to achieve subspaces from the CM. Besides, false peaks appearing in the TOPS and SQ-TOPS spectrums is another problem for these algorithms. The objective of this work was to simultaneously address these two problems. The first problem (i.e., high-complexity) has been tackled through substituting EVD by a computationally-efficient PMs based on a new subsampling methodology. Therefore, one of the most desirable merits of the devised method is low-complexity. The second problem (i.e., false peak generations) has been solved by employing a new evaluation matrix which tested the orthogonality between the transferred SS and the newly created PMs rather than NS. Additionally, the presented methodology to create the PM has made the proposed AOA estimation algorithm to be more robust against coherent sources where the performances of the rival algorithms have deteriorated. The achieved results also showed that the suggested algorithm is much faster than its competitors in localizing wideband sources. These preferable features make the proposed algorithm to be more feasible for limited power and real time applications.

Conflict of Interest

The authors declare no conflict of interest.

Author Contributions

Bakhtiar A. Karim conducted the conceptualization, programing, data analysis, writing - original draft, writing - review & and editing. Prof. Dr Haitham K. Ali was responsible of supervision and results validations.

References

[1] D. Grenier, B. Elahian, and A. Blanchard-Lapierre, "Joint delay and direction of arrivals estimation in mobile communications," *Signal, Image and Video Processing,* vol. 10, no. 1, pp. 45-54, 2016.

[2] W. Chen, X. Zhang, L. Xu, and Q. Cheng, "Successive DSPE-based coherently distributed sources parameters estimation for unmanned aerial vehicle equipped with antennas array," *Physical Communication,* vol. 32, pp. 96-103, 2019.

[3] A. Barnawi, A. Al-Barakati, A. Khan, F. Bajaber, and O. Alhubaiti, "A proposed architecture for a heterogeneous unmanned aerial vehicles system," *Int. J. Electr. Electron. Eng. Telecommun.,* vol. 7, no. 3, pp. 119-126, 2018.

[4] K. Gowri and P. Palanisamy, "Two dimensional direction of arrival estimation algorithm for coherent signals using three parallel uniform linear arrays," *Journal of Communications Technology and Electronics,* vol. 64, no. 12, pp. 1383-1390, 2019.

[5] L. F. Abdulrazak, "I-MUSIC algorithm and fixed null insertion," in *Coexistence of IMT-Advanced Systems for Spectrum Sharing with FSS Receivers in C-Band and Extended C-Band*: Springer, 2018, pp. 81-102.

[6] F. Athley, "Asymptotically decoupled angle-frequency estimation with sensor arrays," in *Proc. Thirty-Third Asilomar Conf. on Signals, Systems, and Computers (Cat. No.CH37020)*, Pacific Grove, CA, USA, 1999, vol. 2, pp. 1098-1102.

[7] J. Cadzow, "A high resolution direction-of-arrival algorithm for narrow-band coherent and incoherent sources," *IEEE Trans. on Acoustics, Speech, Signal Processing,* vol. 36, no. 7, pp. 965-979, 1988.

[8] Y. S. Yoon, L. M. Kaplan, and J. H. McClellan, "TOPS: New DOA estimator for wideband signals," *IEEE Trans. on Signal processing,* vol. 54, no. 6, pp. 1977-1989, 2006.

[9] B. Bilgehan and A. Abdelbari, "Fast detection and DOA estimation of the unknown wideband signal sources," *International Journal of Communication Systems,* vol. 32, no. 11, p. e3968, 2019.

[10] T. E. Tuncer, T. K. Yasar, and B. Friedlander, "Narrowband and wideband DOA estimation for uniform and nonuniform linear arrays," in *Classical and Modern Direction-of-Arrival Estimation*, Elsevier, 2009, pp. 125-160.

[11] M. Wax, T. J. Shan, and T. Kailath, "Spatio-temporal spectral analysis by eigenstructure methods," *IEEE Trans. on Acoustics, Speech, and Signal Processing,* vol. 32, no. 4, pp. 817-827, 1984.

[12] H. Wang and M. Kaveh, "Coherent signal-subspace processing for the detection and estimation of angles of arrival of multiple wide-band sources," *IEEE Trans. on Acoustics, Speech, and Signal Processing,* vol. 33, no. 4, pp. 823-831, 1985.

[13] S. Valaee and P. Kabal, "Wideband array processing using a two-sided correlation transformation," *IEEE Trans. on Signal processing,* vol. 43, no. 1, pp. 160-172, 1995.

[14] E. D. D. Claudio and R. Parisi, "WAVES: Weighted average of signal subspaces for robust wideband direction finding," *IEEE Trans. on Signal Processing,* vol. 49, no. 10, pp. 2179-2191, 2001.

[15] Y.-S. Yoon, *Direction-of-arrival Estimation of Wideband Sources Using Sensor Arrays*, Georgia Institute of Technology, 2004.

[16] K. Okane and T. Ohtsuki, "Resolution improvement of wideband direction-of-arrival estimation" Squared-TOPS"," in *Proc. IEEE International Conf. on Communications*, Cape Town, South Africa, May 2010, pp. 1-5.

[17] H. Hayashi and T. Ohtsuki, "DOA estimation for wideband signals based on weighted Squared TOPS," *EURASIP Journal on Wireless Communications and Networking,* vol. 2016, no. 1, pp. 1-12, 2016.

[18] F. Ma and X. Zhang, "Wideband DOA estimation based on focusing signal subspace," *Signal, Image and Video Processing*, vol. 13, no. 4, pp. 675-682, 2019.

[19] H. Chung, Y. Mi Park, and S. Kim, "Wideband DOA estimation on co-prime array via atomic norm minimization," *Energies,* vol. 13, no. 12, p. 3235, 2020.

[20] X. Qiang, Y. Liu, Q. Feng, Y. Zhang, T. Qiu, and M. Jin, "Adaptive DOA estimation with low complexity for wideband signals of massive MIMO systems," *Signal Processing,* vol. 176, 2020.

[21] N. Hu, T. Wang, Q. Wei, and J. Hu, "Underdetermined wideband DOA estimation utilizing noncircular complex gaussian distribution," *IEEE Sensors Letters*, vol. 4, no. 5, pp. 1-4, 2020.

[22] H. Wu, Q. Shen, W. Liu, and W. Cui, "Underdetermined low-complexity wideband DOA estimation with uniform linear arrays," in *Proc. IEEE 11th Sensor Array and Multichannel Signal Processing Workshop (SAM)*, Hangzhou, China, 2020, pp. 1-5.

[23] A. Asadzadeh, S. M. Alavi, M. Karimi, and H. Amiri, "Coherent wide-band signals DOA estimation by the new CTOPS algorithm," *Multidimensional Systems and Signal Processing*, pp. 1-15, 2020.

[24] A. Abdelbari and B. Bilgehan, "PESO: Probabilistic evaluation of subspaces orthogonality for wideband DOA estimation," *Multidimensional Systems and Signal Processing*, vol. 32, no. 2, pp. 715-746, 2021.

[25] C.-C. Yeh, "Projection approach to bearing estimations," *IEEE Trans. on Acoustics, Speech, and Signal Processing*, vol. 34, no. 5, pp. 1347-1349, 1986.

[26] A. K. Shaw, "Improved wideband DOA estimation using modified TOPS (mTOPS) algorithm," *IEEE Signal Processing Letters*, vol. 23, no. 12, pp. 1697-1701, 2016.

[27] M. A. G. Al-Sadoon, M. D. Ree, R. A. Abd-Alhameed, and P. S. Excell, "Uniform sampling methodology to construct projection matrices for angle-of-arrival estimation applications," *Electronics*, vol. 8, no. 12, p. 1386, 2019.

[28] M. A. G. Al-Sadoon, M. F. Mosleh, N. T. Ali, H. S. Migdadi, R. A. Abd-Alhameed, and P. S. Excell, "Construction of projection matrices based on non-uniform sampling distribution for aoa estimation," *IEEE Access*, vol. 8, pp. 98369-98382, 2020.

[29] J. Zhang, J. Dai, and Z. Ye, "An extended TOPS algorithm based on incoherent signal subspace method," *Signal Processing*, vol.

90, no. 12, pp. 3317-3324, 2010.

[30] B. Li, S. Wang, J. Zhang, X. Cao, and C. Zhao, "Fast randomized-MUSIC for mm-wave massive MIMO radars," *IEEE Trans. on Vehicular Technology*, vol. 70, no. 2, pp. 1952-1956, 2021.

Bakhtiar A. Karim was born in 1989. He received his B.Sc. degree in communications engineering from Sulaimani Polytechnic University (SPU), Iraq, in 2010, and M.Sc. degree in communications and signal processing from University of Leeds, UK, 2016. In 2014, he achieved a scholarship from the Higher Committee for Education Development (HCED), Iraq, to complete the M.Sc. degree. Since 2012, he has been with the communications engineering department, SPU, Iraq, where he is currently a Ph.D. student and lecturer. In 2020, he received a formal HCIA-5G Certificate from Huawei Company and he is currently a formal instructor for that company to deliver 5G courses. His current research interest is mainly focused on angle of arrival estimation algorithms, array signal processing, and antenna design for 5G.

Haitham K. Ali was born in 1970. He received his M.Sc. and Ph.D. degrees from the university of technology, Al-Rashied college of Engineering & science, Baghdad, Iraq, in 1997 and 2006, respectively. He is now a professor in electronics and communication engineering with the technical college of Engineering/ Sulaimani Polytechnic University (SPU). He is the author of several academic journal papers. His research interests are mainly focused on FPGA, electronics and communication, and digital signal processing